INL/CON-13-28098
PREPRINT

Synergistic Smart Fuel for In-pile Nuclear Reactor Measurements

Global 2013

James A. Smith
Dale K. Kotter

October 2013

The INL is a
U.S. Department of Energy
National Laboratory
operated by
Battelle Energy Alliance

Synergistic Smart Fuel for In-pile Nuclear Reactor Measurements

James A. Smith, and Dale K. Kotter, Idaho National Laboratories
Randall A. Ali, Steven L. Garrett, Penn State Graduate Program in Acoustics

INTRODUCTION AND MOTIVATION

In March 2011, an earthquake of magnitude 9.0 on the Richter scale struck Japan with its epicenter on the northeast coast, near the Tōhoku region. In addition to the immense physical destruction and casualties across the country, several nuclear power plants (NPP) were affected.[1] It was the Fukushima Daiichi NPP that experienced the most severe and irreversible damage. The earthquake brought the reactors at Fukushima to an automatic shutdown and because the power transmission lines were damaged, emergency diesel generators (EDGs) were activated to ensure that there was continued cooling of the reactors and spent fuel pools.[2] The situation was being successfully managed until the tsunami hit about forty-five minutes later with a maximum wave height of approximately 15 m.

The influx of water submerged the EDGs, the electrical switchgear, and dc batteries, resulting in the total loss of power to the reactors.[2] At this point, the situation became critical. There was a loss of the sensors and instrumentation within the reactor that could have provided valuable information to guide the operators to make informed decisions and avoid the unfortunate events that followed. In the light of these events, we have developed and tested a potential self-powered thermoacoustic system, which will have the ability to serve as a temperature sensor and can transmit data independently of electronic networks. Such a device is synergistic with the harsh environment of the nuclear reactor as it utilizes the heat from the nuclear fuel to provide the input power.

THERMOACOUSTIC FUEL-ROD RESONATOR

The concept of thermoacoustics, which exploits the interaction between heat and sound waves, offers an attractive solution for the development of a novel, self-powered sensor system. A device known as a thermoacoustic engine produces a sound wave from heat flowing from a high temperature thermal reservoir to a colder one.

Such a device can utilize the high heat energy from a nuclear reactor and convert this into an acoustic oscillation, whose frequency can be correlated to the temperature within the reactor. Figure 1 provides a closer look at this idea.

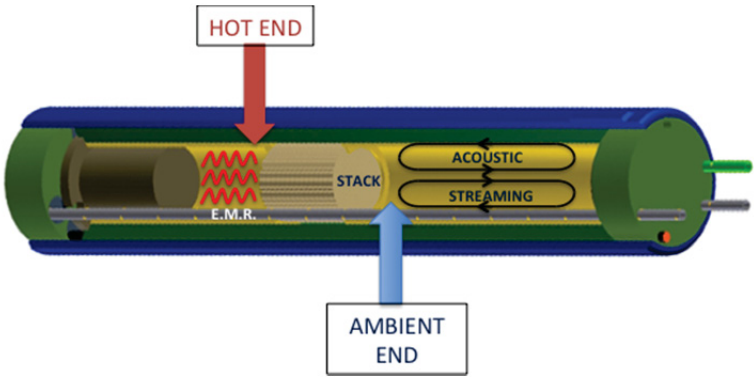

Figure 1. Nuclear fuel-rod adapted to a thermoacoustic sensor. The fuel (left) heats the hot end of the "stack" by electromagnetic radiation. The heat transfer from the ambient-temperature end of the stack is enhanced by the acoustically-driven streaming gas flow indicated by the oblong arrows. That streaming also increases the heat transfer from the gas to the surrounding coolant.

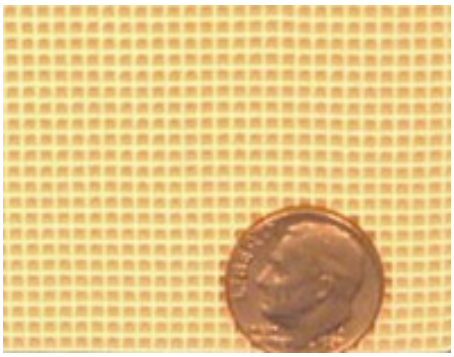

Figure 2. This photograph of the Celcor® ceramic "stack" material is an extruded ceramic used as a substrate for catalytic converters in automotive exhaust systems. This sample has 400 cells/in^2. In the experiment we used 1,100 cells/in^2.

The cylindrically shaped object in Fig. 1 represents a typical nuclear fuel rod, which contains a nuclear fuel source toward the left of the schematic. A nuclear fuel rod happens to behave as a half-wavelength acoustical standing-wave resonator as there is nothing else in the volume enclosed except for the nuclear fuel source. To facilitate the thermoacoustic process, a material known as a "stack" is inserted into the fuel rod. The stack used in our experiments is manufactured from a ceramic and consists of a regular array of parallel pores. Figure 2 is a photograph of such an array of parallel channels. These stacks are manufactured as the substrate for catalytic converters, found in most automotive exhaust systems that convert noxious emissions into carbon dioxide, nitrogen and water vapor.[3] The stack facilitates the transfer of heat to the gas in the resonator in a way that enables the flow of some of that heat to produce sound when there is a temperature gradient along the stack.[4]

For this thermoacoustic sensor, the heat source will be the nuclear fuel, and through electromagnetic radiation (E.M.R.), this heat will reach the hot end of the stack. The ambient side of the stack is initially kept cool from the surrounding cooling fluid and this temperature gradient across the stack will produce acoustic oscillations. When the acoustic wave is generated, a phenomenon known as acoustic streaming[4] will occur on the other side of the stack, *i.e.,* the ambient end (right of Fig. 1). This acoustic streaming is a convective jet of gas, which will circulate hot gas away from the heat source (nuclear fuel) and along the walls of the engine and then into the surrounding cooling fluid, as depicted by the arrows in Fig. 1. This will reduce the temperature of the ambient end of the stack, maintaining the temperature gradient needed for sustained acoustic oscillations.

There is a simple relationship between the frequency of the sound, the speed of the sound within the resonator, and the temperature of the gas within the resonator. Utilizing these relationships, it is possible to establish a clear, accurate correlation of the temperature within the nuclear fuel rod to the frequency of the sustained oscillation. This frequency is propagated by sound radiation throughout the cooling fluid in the reactor and can monitored at a remote location.

This solution is simple and synergetic with the harsh operation conditions of the nuclear reactor. There are no physical moving parts required for the device, there are no heat exchangers required for operation, no in-pile cabling requirements and the sensor is self-powered as it uses the nuclear fuel for its heat source. Integrating such sensor systems along with the existing nuclear reactor instrumentation can prove to be a significant benefit for the nuclear industry.

For our feasibility study, Idaho National Laboratories manufactured a nuclear fuel rod, 21.5 cm long machined from Nitronic 60 Stainless Steel. The fuel rod was adapted to a thermoacoustic engine by insertion of a stack, whose parameters were designed with DELTAEC.[5] The thermoacoustic fuel-rod resonator was fully instrumented to measure pressures and temperatures along the resonator. Additionally, since nuclear fuel was not available for these experiments, indirect heating strategies were applied and the device was submerged in a large water bath, which acted as the surrounding cooling fluid of a fuel-rod in a nuclear reactor. Further details on the experiments and instrumentation have been discussed in previously published work by the authors.[6,7]

THERMOMETRY

The well-known equation relating the pressure-independent speed of sound, c, in an ideal gas demonstrates that c is proportional to the square root of the absolute (Kelvin) temperature of the gas, T. In equation 1(a), $\mathfrak{R}$ = 8.314471 J/mole-K is the Universal Gas Constant, $\gamma = c_p/c_v$ is the polytropic coefficient, which is the ratio of the specific heat at constant pressure to that at constant volume. For dry air γ = 1.403 and M = 0.02897 kg/mole is the mean molecular weight.[8] For a half-wavelength resonator, such as the thermoacoustic fuel-rod resonator described, the frequency of the first longitudinal mode of vibration, f, is related to the speed of sound by $c = 2Lf$, where L is the length of the resonator. Hence it is possible to derive an invariant expression from the ratio of this frequency to the square root of the temperature of the gas as shown in equation 1(b).

$$c = \sqrt{\frac{\gamma \mathfrak{R} T}{M}} \qquad (1a)$$

$$\frac{f}{\sqrt{T}} = \frac{1}{2L}\sqrt{\frac{\gamma \mathfrak{R}}{M}} \qquad (1b)$$

An additional complexity is associated with these simple equations in their application to the

thermoacoustic fuel-rod resonator since the thermoacoustic resonator does not have a constant temperature throughout. The cross-sectional area of the duct changes (slightly) in the region where the stack partially occludes the resonator. Also, a substantial temperature gradient across the stack of approximately 400 ^{o}C to 450 ^{o}C is required for operation and there are no hot or cold heat exchangers so the temperature is less spatially uniform in the hot duct side of the stack or the ambient temperature duct on the other side of the stack. For equation 1(b) to be applied in this more complicated situation, an effective sound speed c_{eff} must be defined. It is determined by an effective temperature T_{eff} of the gas at some location within the resonator. The thermoacoustic oscillation can be thought of as averaging the spatially-varying temperature throughout the resonator, thus determining its resonance frequency and the dependence of that frequency on an effective temperature. A model will be developed to arrive at this averaged temperature that the frequency is "measuring".

To investigate the relationship between the effective temperature in the resonator and the fundamental frequency, the temperature profile of the gas in the resonator was measured using four thermocouples and one integrated circuit temperature sensor (AD 592). The locations of these temperature measurements along the resonator are shown in Fig. 3 (left). A piezoresistive microphone was also included to measure the acoustic pressure and frequency.

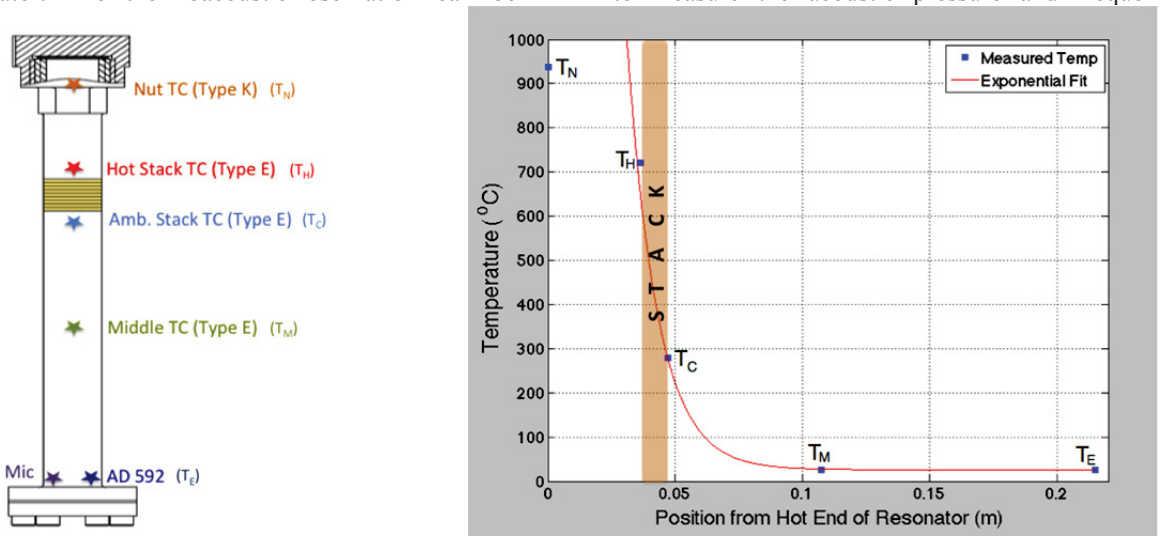

Figure 3. (Left) The thermoacoustic resonator instrumented with several thermocouples and an integrated-circuit temperature sensor to measure the longitudinal temperature profile along the resonator, as well as a piezoresistive pressure sensor that measured the static gas pressure and acted as a microphone for measurement of the acoustic (dynamic) pressure. (Right) The spatial variation of the mean temperature across the resonator at a particular time is sampled by the five temperature sensors within the resonator. The line is an exponential fit to those measured temperatures from the hot end of the stack (T_H) to the ambient rigid end of the resonator, (T_E), that is used in the 31-segment model of Fig. 4.

While the system was in operation, the temperature and frequency information was acquired every two minutes. Figure 3 (right) shows the typical measured temperature profile of the thermoacoustic resonator. The temperature at the location of the simulated fuel source (or nut temperature, T_N) was between 900 ^{o}C and 1,000 ^{o}C. The remainder of the temperature profile along the resonator is reasonably well-approximated with an exponential fit as shown by the solid line in Fig. 3 (right).

Using this information, a transfer matrix network was developed to characterize the temperature-frequency relationship of the thermoacoustic sensor. A transfer matrix network utilizes lumped elements to represent small sections or slices of the resonator, which take into consideration the longitudinal variation in temperature in the gas in the resonator as well as changes in the cross sectional area due to the stack. These lumped elements are very short compared to the wavelength of sound and represent simple mechanical or electrical topologies, which can be used to analyze an acoustical system (or vice-versa). Acoustical inertances, L_{acs} (masses/inductors), and acoustical compliances, C_{acs} (springs/capacitors) are the lumped elements that were used for this transfer matrix network. C_{acs} is not affected by temperature changes since it is dependent on the mean gas pressure. On the other hand, L_{acs} is density dependent and in turn temperature dependent. Since the static pressure is spatially uniform within the

resonator, the local temperature of the gas determines its local mass density.

Figure 4 shows the division of the resonator (with cross sectional area, A) into 31 slices. One slice represents the hot duct area from the hot end of the resonator (location of nuclear fuel) to the hot end of the stack, 10 slices represent the region of the stack and the remaining 20 slices represent the length from the ambient end of the stack to the ambient rigid end of the resonator.

Each slice is represented by a lumped element network, consisting of an inertance flanked by two half-compliances, as shown in Fig. 4. These lumped element networks across the length of the resonator will be sequentially multiplied, resulting in a transfer network matrix that relates the pressure, p_1 and volume velocity, U_1 on one side of the resonator to the pressure, p_2 and volume velocity, U_2 on the other side. The static pressure obtained from the microphone was used in the calculation of C_{acs} and the temperature profile of the resonator was used in the calculation of L_{acs}. In Fig. 4, the average of T_N and T_H (recall Fig. 3 (Left)) was used to represent the temperature of the hot duct. The exponential fit to the temperature profile was used to calculate the temperature of each of the remaining slices, and hence an inertance for each of those sections.

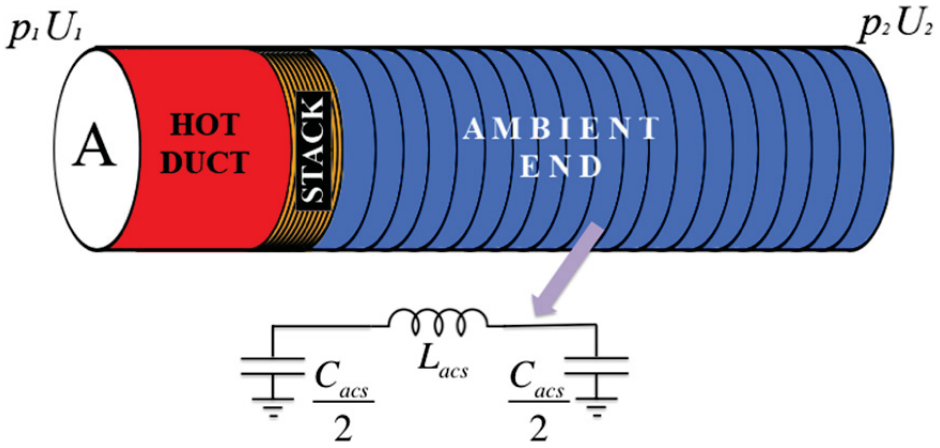

Figure 4. The 31-slice model of the resonator to which the transfer matrix was applied. A represents the cross-sectional area of the tube. p_1, U_1, p_2, and U_2 are pressures and volume velocities of the gas on either end. The first slice is used to represent the hot duct at a constant temperature. The exponential temperature profile was applied to the remaining slices, 10 of which are dedicated to the stack and 20 to the ambient end of the resonator. Each slice was represented by a lumped element network of an inertance, L_{acs}, flanked by two half compliances, $C_{acs}/2$.

The transfer matrix was solved[6] to find a modeled frequency for each temperature profile that was captured (every two minutes during the operation of the resonator). This modeled frequency, along with the measured frequency as a function of the temperature at the middle of the resonator, T_M, is shown in Fig. 5. It can be seen that the model is approximating the frequency quite well. Although the initial part of the graph in Fig. 5 does not seem to correlate well by eye, it represents a difference of only 1%.

In practice, if this thermoacoustic fuel-rod resonator were to be used as a temperature sensor, the only output information that would be available to an operator would be the frequency. Utilizing equation 1(b), this frequency can be used to calculate a corresponding temperature somewhere along the length of the resonator. This temperature will not be the temperature of the middle of the resonator, but rather an effective temperature along the resonator.

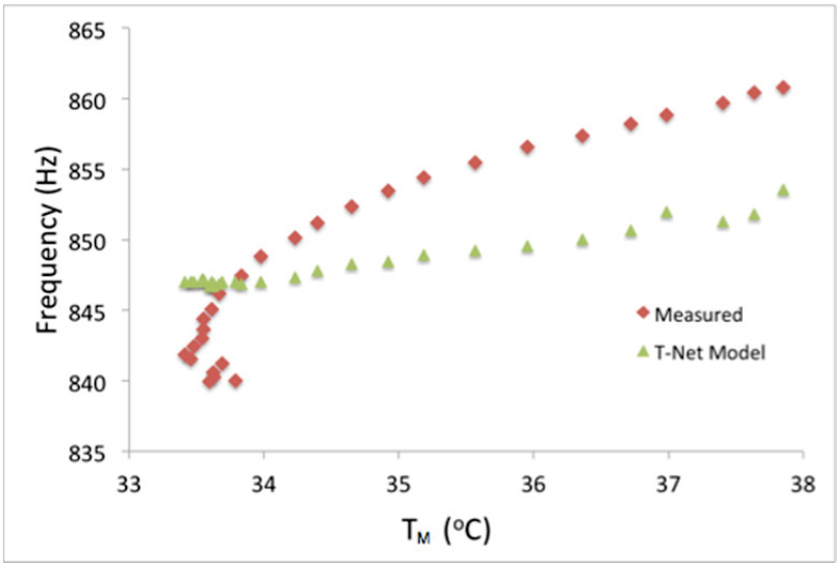

Figure 5. Measured and transfer matrix modeled frequencies as a function of the temperature T_M at the centre of the resonator. Note that the discrepancy between the frequencies is only about 1%.

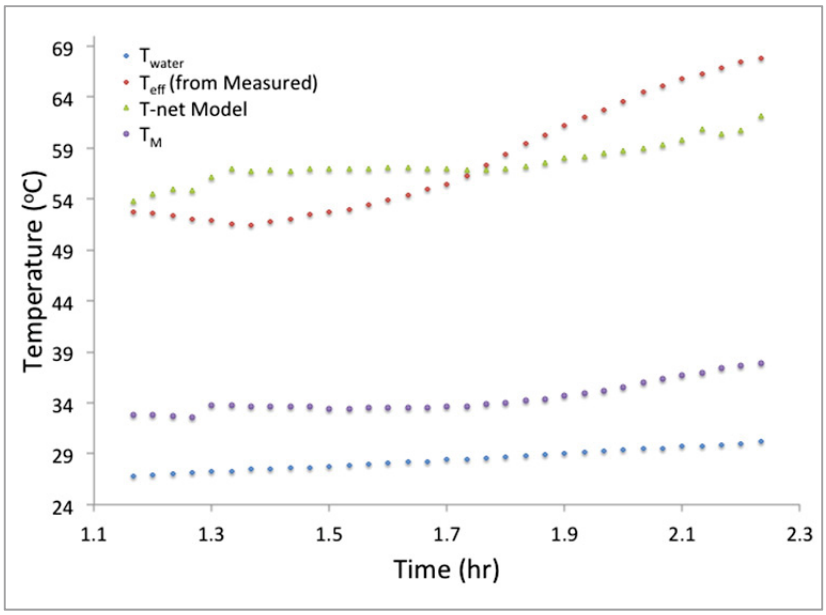

Figure 6. The effective temperature from the measured frequency (T_{eff}, **red**), the temperature at the centre of the resonator (T_M, **purple**), the water temperature (T_{water}, **blue**) and the T-Network modeled temperature (T-net, **green**) during an indirect run of the resonator. After 1.7 hours, the system began to lose acoustics due to a gas leak; note the divergence of the middle gas temperature from the water temperature indicating reduction of thermal contact.

Figure 6 shows this effective temperature from the measured frequencies, T_{eff}, along with the temperature calculated from the transfer matrix model, the temperature at the middle of the resonator, T_M, and the water temperature, T_{water}. Observing the temperature profile of the resonator in Fig. 3 (right), it can be seen that the measured effective temperature lies between T_C and T_M, but closer to T_M, hence it can be taken as a representation of the effective temperature of the ambient end in the fuel-rod.

The effective temperatures obtained from the T-Network model were within ± 8 °C of the measured effective temperatures. Clearly, one of the main approximations in the model was the exponential fit to the temperature based on only four thermocouple measurements. Additionally, this model did not represent any azimuthal temperature variations. It was assumed that within any slice the temperature was the same from the walls of the resonator to the center of the resonator. This is not a necessarily bad assumption since there is an improved thermal contact between the gas within the resonator and the water in the presence of acoustic streaming (see Fig 9 (right)).

By logarithmic differentiation of Eq. 1(b), the sensitivity of the thermoacoustic sensor in this work can also be evaluated. The temperature uncertainty δT is related to the uncertainty in the frequency δf.

$$\delta T = \frac{2T}{f}\delta f \tag{2}$$

In the experiments described in this section, the frequencies were measured to ± 0.01 Hz, resulting in very small relative uncertainty in the temperature. For the results in Figs. 5 and 6, $f \cong 850$ Hz and $T \cong 350$ K so an uncertainty in frequency of ±0.01 Hz corresponds to an uncertainty in temperature of about ±0.01 °C; a differential sensitivity of about $(dT/df) = 0.8$ K/Hz. As was discussed earlier, although small changes in temperature can be tracked very accurately, the relationship between the measured frequency and a temperature in a particular location within the resonator or the fluid surrounding the resonator can be difficult to establish to better than 5%.

Our frequency measurements were made using a high sensitivity piezoresistive microphone, which is not available at the site of the nuclear reactor. Naturally, this leads to one of the other important concerns, which the future work of this technology would address: effective and reliable methods to measure the frequency of the sound propagated throughout the nuclear reactor. Current ideas that have been put forth include wireless hydrophones and robots to measure the sound.

Another consideration for this sensor strategy is its operating temperature range. The equipment used for the experiments was limited in the capability to reach temperatures beyond 1,000 °C. However, the Celcor® stack material (see Fig. 2) can operate up to a temperature of 1,200 °C and withstand spikes up to 1,400 °C, which provides a physical limit for this particular thermoacoustic sensor. However, other porous media that can be used as a stack may provide higher operating temperatures. One example is reticulated vitreous carbon, which has a temperature limitation of 3,500 °C in an oxygen-free atmosphere.[9]

In addition to thermoacoustic sensor having the capability to measure an effective temperature, it is not inconceivable to use this technology to probe different parts of the nuclear reactor, in particular the surrounding cooling fluid or graphite capsules used to house fuel stacks in gas-cooled reactors. There is an improved thermal contact between the gas within the resonator and the surrounding cooling fluid when there are acoustic pressure oscillations present. Consequently, it is possible to infer the surrounding cooling fluid's temperature from the effective temperature of the gas within the fuel rod (see Fig. 9 (right)). Additionally, the high temperatures of graphite capsules in nuclear reactors can be another source of heat to drive a thermoacoustic engine into onset. The stack location can also be changed within the thermoacoustic sensor, so that the effective temperature is representative of a different section of the resonator.

MONITORING OF GASEOUS ISSION PRODUCTS

We believe that this thermoacoustic strategy can be extended to self-powered remote sensing of changes in fuel porosity and to tracking of fission gas (particularly krypton and xenon) evolution as part of the radioactive decay of the fuel.[10] Although, in such separate effects, pairs of fuel-rod resonators may be required (*e.g.,* one to measure temperature and the other to identify gas mixture concentration). Sound speed measurements have already been used successfully to measure the isotopic ratios of ^{3}He to ^{4}He,[11] and initial results performed at the INL confirm the practicality for the fission gas application as shown in Table I. Experimental results show that resonance frequency is directly correlated to the ratio of the square root of the polytropic coefficient $\gamma = c_P/c_V$ to the mean molecular mass M of the gases as shown in Eq. (1). Varying the gas within the TAC results in changes in the frequency and the amplitude of the sound radiated. The measured frequency ratios are not exactly equal to those based on the properties of the gases due to the fact that the temperatures during all four measurements were nearly but not exactly equal and the humidity of the air sample was unknown.

Gas	Molecular Mass (a.m.u.)	Polytropic Coefficient ($\gamma = c_P/c_V$)	Ave. Freq. (Hz)	Freq. Ratio f/f_{He}	Sq. Root (Mass/γ) Ratio
Helium	4.00	1.667	976.2	1.000	1.000
Nitrogen	28.01	1.400	315.7	0.323	0.346
(Dry) Air	28.96	1.403	322.7	0.331	0.341
Xenon	131.29	1.667	173.0	0.177	0.175

Table I. Summary of the measured resonance frequency for four different gases used to generate thermoacoustic standing waves in the same resonator. The ratio of the measured frequencies to the measured frequency with helium is compared to the ratio calculated using the molecular mass M and the ratio of specific heats, $\gamma = c_P/c_V$.

HEAT TRANSFER ENHANCEMENT

The measurements presented thus far were made in the calorimeter shown in Fig. 8. The heat transfer paths are also important to recognize in this device, as they are required for keeping this sensor in continuous operation. Figs. 7 and 8 shows the different paths through which heat is transferred from the heat source (nuclear fuel) to the hot and ambient ends of the stack, into the water and ultimately into the surrounding environment. The dominant method of heat transfer from the heat source to the hot end of the stack is electromagnetic radiation, Q_{rad}. Q_{resw} is the conductive heat flow from the heat source that entirely bypasses the gas, but alternatively flows through the walls of the resonator and into the water. The heat from the hot end of the stack can be transported to the ambient end of the stack through a conductive path, Q_{ha}. Another conductive heat flow path also exists from the ambient end of the stack to the walls of the resonator and into the water, Q_{aw}.

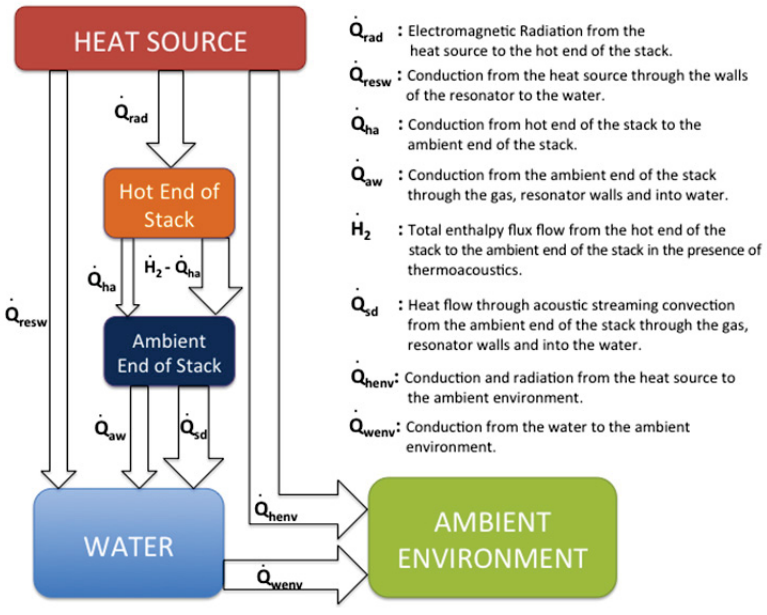

Figure 7. Heat transfer flow paths from the thermoacoustic fuel-rod resonator contained within the calorimeter shown in Fig. 8.

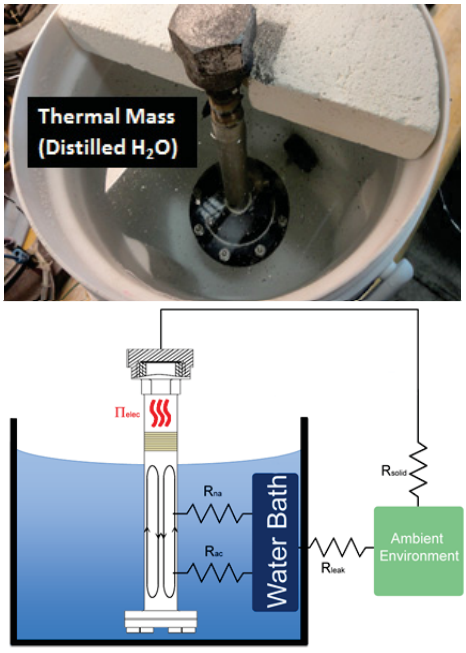

Figure 8. (Above) View into the water-filled calorimeter with one half of the insulated lid removed. (Below) Schematic representation of the heat flow paths and corresponding resistances.[7]

With the thermoacoustic effect present within the resonator, there are two primary effects that contribute to the heat transfer: *(i)* enthalpy transport along the stack due to the "bucket brigade" effect[12] which acoustically transports heat through the stack and *(ii)* enhanced thermal contact between the acoustically-oscillating gas and the walls of the resonator due to acoustically-driven streaming (Q_{sd} in Fig. 7).[13,14] The total power flowing through the stack, which includes Q_{ha} is denoted by H_2 (Ref. 4), hence in Fig. 7, this enthalpy transport from the hot end of the stack to the ambient end of the stack due to thermoacoustics alone is $H_2 - Q_{ha}$. The remaining heat flow paths in Fig. 7, Q_{henv} and Q_{wenv} are the heat losses from the heat source and the water to the ambient environment.

To understand the thermoacoustic heat transfer effects, experiments were done using a linear actuator to control the suppression and reactivation of acoustic oscillations within the fuel-rod resonator.[7] Figure 9 (left) shows the temperature of the ambient end of the stack with and without the presence of acoustic oscillations. In relation to Fig. 7, this corresponds to the introduction of the parallel heat flow path $H_2 - Q_{ha}$ when there are acoustic oscillations in the resonator. $H_2 - Q_{ha}$ continuously drives more heat from the hot end of the stack to the ambient end of the stack, lowering the temperature at the hot end of the stack and increasing the temperature of the ambient end of the stack as shown in Fig. 9 (Left). Hence, there is a greater temperature difference between the heat source and the hot end of the stack. Since the electromagnetic radiation from the heat source to the hot end of the stack is proportional to the fourth power of their absolute (Kelvin) temperatures, Q_{rad} will increase.

At the same time, the heat that is being accumulated on the ambient end of the stack is continuously being removed by the acoustically-driven streaming convection, Q_{sd}, and deposited onto the walls of the resonator and ultimately into the water. This maintains the temperature gradient across the stack for continued operation of the thermoacoustic sensor. Figure 9 (right) shows the temperature of the water (blue) and the temperature of the gas at the centre of the resonator, with and without acoustic oscillations (red). It is quite evident that there is an improved thermal contact as the temperature of the gas is reduced closer to the water temperature when there are sustained acoustic oscillations. It has also been demonstrated through these heat transfer experiments that the velocity of the acoustic streaming is proportional the square of the acoustic pressure amplitude.[7]

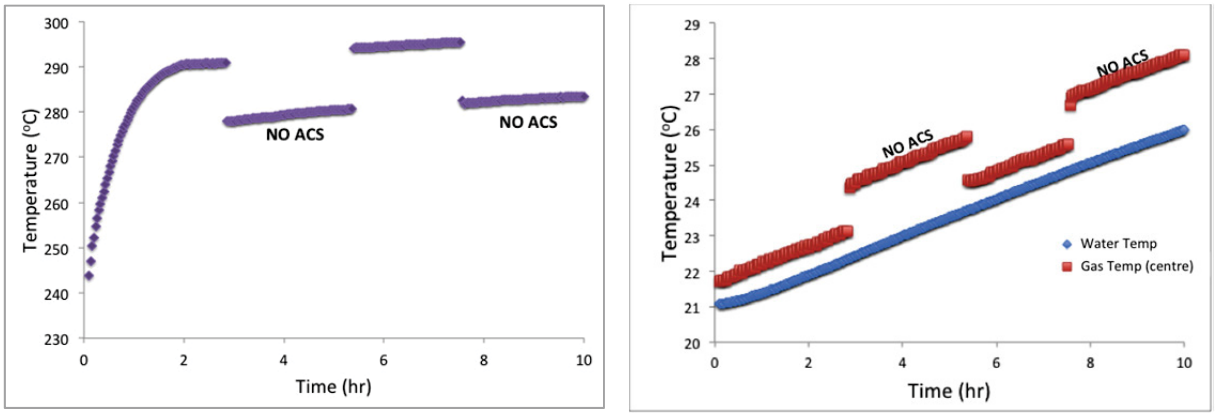

Figure 9. (Left) Temperature of the ambient end of the stack with and without acoustic oscillations (ACS) demonstrating the enhancement of heat flux through the stack due to thermoacoustic effects. (Right) Temperature at the centre of the resonator and of the surround cooling water, with and without acoustic oscillations. This demonstrates an enhanced thermal contact between the gas and the water when the fuel rod supports and acoustic standing wave.

CONCLUSIONS

The thermoacoustic fuel rod sensor developed in this research has demonstrated a novel technique for monitoring the temperature within the core of a nuclear reactor or the temperature of the surrounding heat-transfer fluid. It uses the heat from the nuclear fuel to generate sustained acoustic oscillations whose frequency will be indicative of the temperature. Converting a nuclear fuel rod into this type of thermoacoustic sensor simply requires the insertion of a porous material (stack). This sensor has demonstrated a synergy with the elevated temperatures that exist within the nuclear reactor using materials that have only minimal susceptibility to high-energy particle fluxes.

When the sensor is in operation, the sound waves radiated from the fuel rod resonator will propagate through the surrounding cooling fluid. The frequency of these oscillations is directly correlated with an effective temperature within the fuel rod resonator. For this half-wavelength thermoacoustic resonator, the effective temperature is more representative of the ambient section in the fuel rod (from the ambient end of the stack to the ambient rigid of the fuel rod), than the temperature of the nuclear fuel. In such a design, utilizing a look up table of exponential fits that correlate to the effective temperature, may allow for the extraction of the temperature profile of the entire fuel rod from the hot end of the stack to the ambient rigid end. However, this is an idea that is yet to be fully investigated. It is also worthy to note that a different resonator design could emphasize the temperature in a different location (*e.g.,* the hot end of the stack).

While this thermoacoustic fuel rod sensor has been designed to measure the temperature within the gas of the fuel rod or the surrounding cooling fluid, it is possible to utilize the same technology to measure temperature in other parts of the reactor, such as a graphite capsule or infer the temperature of the surrounding cooling fluid. The frequency and the amplitude of the acoustic oscillations can also provide additional information to use as other types of sensors. For instance, at the Idaho National Laboratories, preliminary experiments have been conducted to use the thermoacoustic effect to measure fuel porosity, molecular mass of the gas within the fuel rod, and to track fission gases.

The effects of the acoustic streaming on this device is also worthy of appreciation. Due to acoustically-forced convective motion of gas, heat is continually removed from the ambient temperature end of the stack and maintains the critical thermal gradient across the stack for continuous operation of this device. It was also shown that acoustic streaming reduced the temperature difference between the middle of the fuel rod and the surrounding water. Since it is has been demonstrated that the amount of heat removed is quadratic with acoustic pressure amplitude, high amplitude acoustic oscillations may help in lowering the temperature at the centre of the fuel rod even further.

Future work will explore various methods to measure the frequency of the sound that is propagated throughout the reactor. However, current ideas that have been put forth are hydrophones and remotely controlled robots. The method of measuring the frequency outside the reactor vessel will likely be able to operate on some reserve power supply such as a battery for this sensor to provide information in emergency situations, such as Fukushima where the main electrical power was lost.

As the implementation of nuclear power is growing globally, it is important that the mechanisms and sensors employed to ensure that a nuclear reactor is within its region of safe operation be continuously refined and revisited. The thermoacoustic fuel rod sensor is representative of this motive and demonstrates an exciting, alternative system to monitor the status within a nuclear reactor, particularly useful in emergency situations.

ACKNOWLEDGMENTS

The authors wish to thank the project sponsors for their support of this work: the U.S. Department of Energy/Nuclear Energy, the U.S. Department of Energy Idaho, the Idaho National Laboratory, and the Battelle Energy Alliance, LLC who administered the grant to Pennsylvania State University. One of us (R.A.A.) would like to acknowledge the support of One of us (R.A.A.) would like to acknowledge the support of the U.S. Fulbright Commission and the Organization of American States for providing graduate fellowship support.

REFERENCES

1. International Atomic Energy Agency Mission Report, International fact finding expert mission of the Fukushima Daiichi nuclear power plant accident following the great east Japan earthquake and Tsunami, May-June 2011.

2. D. KLEIN and M. CORRADINI, "Fukushima Daiichi: ANS Committee Report," *American Nuclear Society* (Revised June 2012). [Online] Available: http://fukushima.ans.org/report/Fukushima_report.pdf.

3. Corning, "Corning ceramic substrates", (1994-2012),

   URL: http://www.corning.com/environmentaltechnologies/products_services/ ceramic_substrates.aspx.

4. G. W. SWIFT, *Thermoacoustics : A unifying perspective for some engines and refrigerators* (Acoustical Society of America through the American Institute of Physics, 2002); ISBN 0735400652.

5. W. C. WARD and G. W. SWIFT, "Design environment for low-amplitude thermoacoustic engines", Journal of the Acoustical Society of America **95**, 3671–3672 (1994). (For latest download: http://www.lanl.gov/thermoacoustics/DeltaEC.html).

6. R. A. ALI, S. L. GARRETT, J. A. SMITH, and D. K. KOTTER, "Thermoacoustic thermometry for nuclear reactor monitoring," IEEE J. Instrumentation & Measurement **16**(3), 18-25 (2013) .

7. R. A. ALI and S. L. GARRETT, "Heat transfer enhancement though thermoacoustically-driven streaming," Proc. Mtgs. Acoust. **19**, 030001 (2003).

8. National Oceanic and Atmosphere Administration, National Aeronautics and Space Administration, United States Air Force, *U.S. Standard Atmosphere*, 1976.

9. J. A. ADEFF, T. J. HOFLER, A. A. ATCHLEY, and W. C. MOSS, "Measurements with reticulated vitreous carbon stacks in thermoacoustic prime movers and refrigerators", Journal of the Acoustical Society of America **104**(1), 1145–1180 (1998).

10. W. M. STACEY, *Nuclear Reactor Physics, 2nd ed.*, (Wienheim: Wiley & Sons Inc., 2007).

11. E. POLTURAK, S. L. GARRETT, and S. G. LIPSON, "Precision acoustic gas analyzer for binary mixtures," Review of Scientific Instruments **57**(11), 2837-2841 (1986).

12. A. GOPINATH, N. L. TAIT, and S. L. GARRETT, "Thermoacoustic streaming in a resonant channel: The time-averaged temperature distribution", Journal of the Acoustical Society of America **103**(3), 1388–1405 (1998).

13. P. VAINSHTEIN, M. FICHMAN, and C. GUTFINGER, "Acoustic enhancement of heat transfer between two parallel plates", International Journal of Heat and Mass Transfer **38**, 1388–1405 (1995).

14. G. PENELET, M. GUEDRA, V. GUSEV, and T. DEVAUX, "Simplified account of Rayleigh streaming for the description of nonlinear processes leading to steady state sound in thermoacoustic engines", International Journal of Heat and Mass Transfer **55**, 6042–6053 (2012).